JOURNAL OF MATERIALS SCIENCE 27 (1992) 1716–1722

Equilibrium thermodynamics of nonstoichiometry in ZnO and aluminium doping of ZnO using aluminium chloride

A. PAUL†, H. N. ACHARYA
Indian Institute of Technology, Kharagpur 721 302, India

A critical assessment of nonstoichiometry that can occur in zinc oxide at various temperatures and oxygen pressures has been made using the concepts of equilibrium thermodynamics. The feasibility of producing transparent conducting films of aluminium-doped zinc oxide by spray pyrolysis of organo-zinc salt solution containing aluminium chloride is also discussed.

1. Introduction

The use of ZnO in modern technology ranges from varistors [1], mixed oxide ferrites (typical nickel–zinc ferrite) [2], pigments, activators for vulcanization of rubber [3], spinels with Al_2O_3 such as gahnite ZnO Al_2O_3, which has interesting refractory properties [4–7]. When combined with 10–15% TiO_2, ZnO yields a product of moderately high electrical conductivity with the ability to absorb radio frequency (microwave) power [8, 9]. The piezoelectric properties of ZnO are of considerable interest because, compared to quartz, the electrochemical coupling in ZnO is large [10]. In photovoltaics and other optoelectronic applications, thin coatings with high transmissivity and low sheet resistance are necessary. For amorphous silicon solar cells, indium tin oxide (ITO) films and tin oxide (SnO_2) films are frequently used as transparent electrodes. Transparent semiconducting ZnO films may be a promising alternative to these materials [11, 12]. These films can also profitably be used in electron photography (electronic faxing) due to its desirable photoconductivity [13, 14].

The influence of impurities and deviation from stoichiometry strongly affects the properties of ZnO in bulk (single crystal/polycrystal) as well as in thin films. For example in an *n*-type semiconductor, oxygen deficiency leads to a marked increase in electrical conductivity, whereas *p*-type characteristics can be achieved with very high oxygen pressure on ZnO [15–18]. A typical example of impurity doping on the electrical conductivity of ZnO is shown in Fig. 1 as a function of temperature.

The non-stoichiometry of compounds in the Zn–O system will depend on the temperature and the fugacity of oxygen during synthesis. In the present paper, a critical assessment of non-stoichiometry that can occur in ZnO at various temperatures and oxygen pressures is presented using the concepts of equilibrium thermodynamics. Recently, attempts have been made to produce transparent conducting films of aluminium-doped ZnO by spray pyrolysis of organozinc solutions containing aluminium salt. Results of typical thermal and other analyses of this system will also be presented.

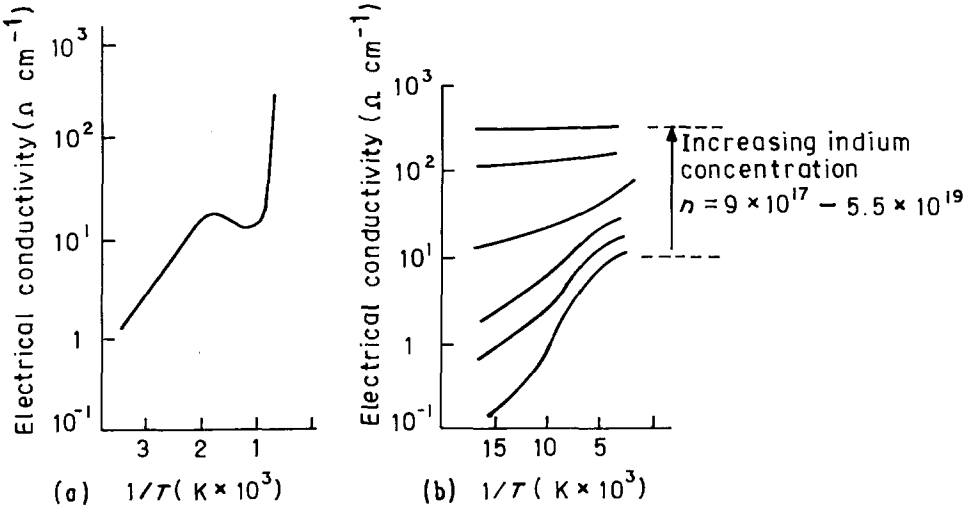

Figure 1 Electrical conductivity of pure and doped zinc oxide. (a) Typical single crystal of zinc oxide (pure, intrinsic); (b) Typical indium-doped single crystals of zinc oxide [15].

† The death of Professor Paul represents a considerable loss to the Materials Science community. His many distinguished contributions to this and other journals stand as a testimony to his outstanding research.

0022–2461

2. Experimental procedures

To prepare zinc acetate crystal, 2.0 g of extra pure ZnO (impurity content less than 2 p.p.m.) was dissolved in a mixture of 20 ml glacial acetic acid and 10 ml deionized water. The clear solution was evaporated on a hot plate (set at 90 °C) until the volume was reduced to two thirds. The solution was air-cooled to room temperature (28 ± 2 °C) and allowed to crystallize for 24 h. The needle-shaped crystals were filtered, repeatedly washed with dry ethyl alcohol, and kept in a vacuum desiccator for 2 h. Part of the dried crystal was finely powdered in an agate mortar and used for thermal analysis with the Stanton Redcroft, UK, STA 781 system. During thermal analysis, the constant heating rate was maintained at 10 °C min^{-1} and a steady stream of dry air was allowed to flow through the cell. The rest of the crystal was used for X-ray and other analyses.

2.0 g of ZnO was also dissolved in a mixture of 20 ml glacial acetic acid, 10 ml deionized water and 0.2 ml of concentrated HCl (~ 12 N). In this case, the solution was evaporated to dryness over a hot plate (set at 90 °C), and then further dried for 4 h in a vacuum desiccator. The residue was sticky even after drying, probably due to the non-crystallinity and hygroscopic nature of the $ZnCl_2$ portion. This powder was also analysed thermally and with X-ray diffraction (XRD) and i.r. spectroscopy (IRS).

3. Results and discussion

3.1. Equilibrium thermodynamics of the Zn–O–Cl and Al–Cl systems

The standard Gibbs free energies of the reactions

$$Zn\,(solid, gas) + \tfrac{1}{2}O_2\,(gas) \rightleftharpoons ZnO\,(solid) \quad (1)$$

and

$$Zn\,(solid, liquid, gas) + Cl_2\,(gas) \rightleftharpoons ZnCl_2\,(solid, liquid, gas) \quad (2)$$

were calculated from available thermochemical data (given in Table I) and are plotted in Fig. 2 as a function of temperature. As expected, the free energy plots change slopes at different phase transition temperatures, i.e. 591 K (mp of $ZnCl_2$), 692.5 K (mp of Zn), 1005 K (bp of $ZnCl_2$) and 1180 K (bp of Zn) under one atmospheric pressure. The free energy of formation of $ZnCl_2$ at all stages is more negative than that of ZnO; the difference between these two free energies reaches the minimum around 1005 K (about 1000 cal mol^{-1}, corresponding to an equilibrium constant ~ 247). Thus in the presence of chloride in a solution of zinc acetate, as used for spray pyrolysis, zinc chloride will be formed in preference to zinc oxide.

TABLE I Standard Gibbs free energies of formation of ZnO and $ZnCl_2$ (in calories)

Zn (solid)	$+ \frac{1}{2}O_2$ (gas) $\rightleftharpoons$ ZnO (solid)	(1)
Zn (gas)	$+ \frac{1}{2}O_2$ (gas) $\rightleftharpoons$ ZnO (solid)	(1a)
Zn (solid)	$+ Cl_2$ (gas) $\rightleftharpoons$ $ZnCl_2$ (solid)	(2)
Zn (solid, liquid)	$+ Cl_2$ (gas) $\rightleftharpoons$ $ZnCl_2$ (liquid)	(2a)
Zn (gas)	$+ Cl_2$ (gas) $\rightleftharpoons$ $ZnCl_2$ (gas)	(2b)

ΔG°_1	$= -84100 - 6.9T\log T + 44.14T$	(298–693 K)
ΔG°_{1a}	$= -115420 - 10.35T\log T + 82.38T$	(1170–2000 K)
ΔG°_2	$= -101385 - 12.85T\log T + 75.45T$	(298–586 K)
ΔG°_{2a}	$= -93950 + 27.35T$	(586–1005 K)
ΔG°_{2b}	$= -93800 - 9.44T\log T + 38.6T$	(1180–1800 K)

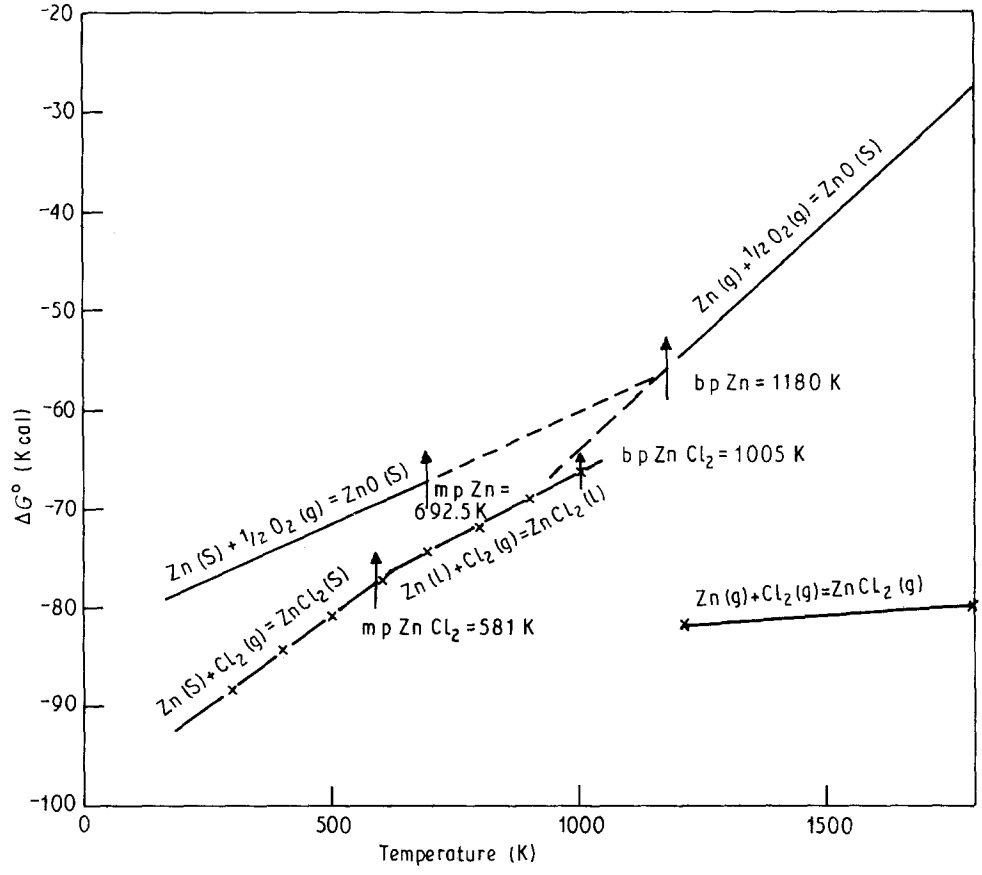

Figure 2 Standard Gibbs free energy of (a) Zn (s, g) + $\frac{1}{2}O_2$ (g) $\rightleftharpoons$ ZnO (s); (b) Zn (s, l, g) + Cl_2 (g) $\rightleftharpoons$ $ZnCl_2$ (s, l, g).

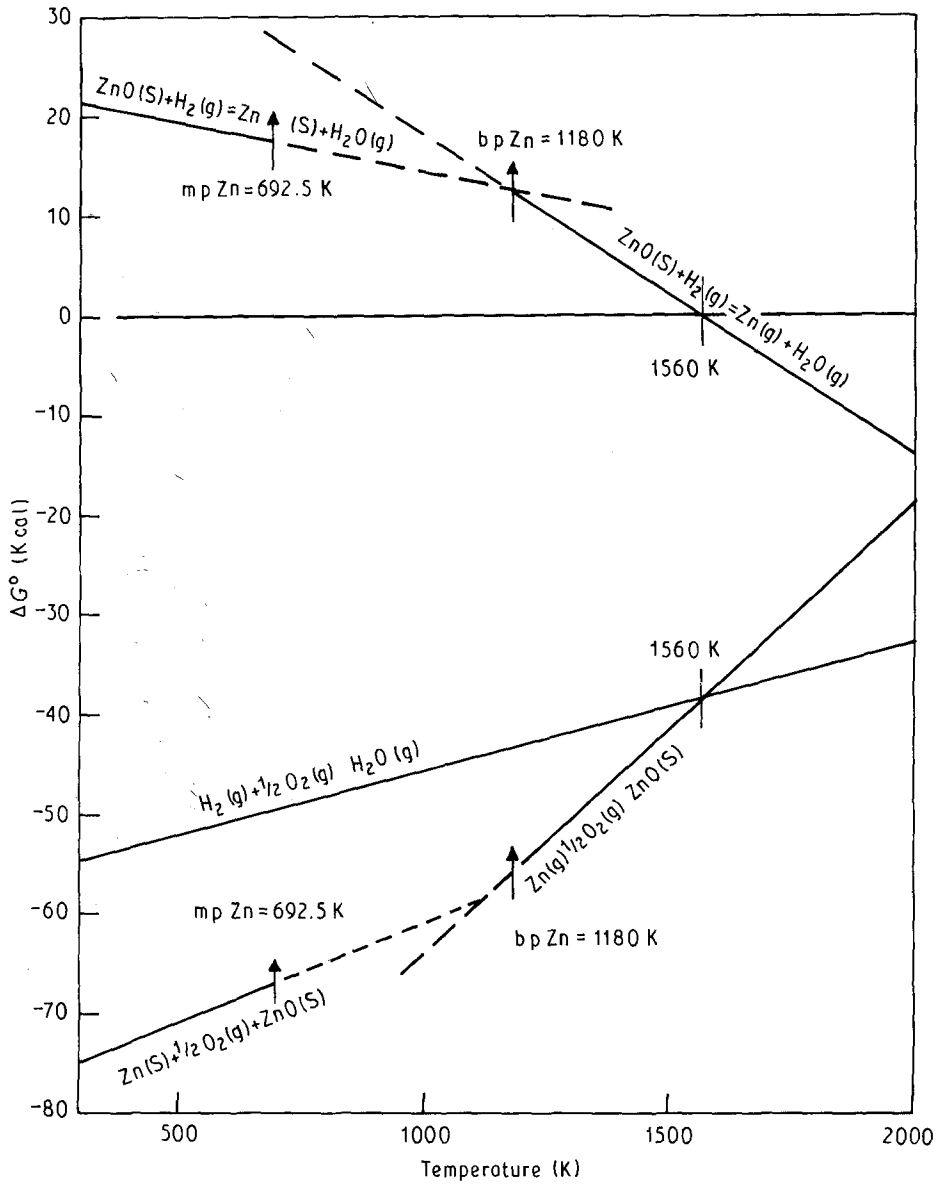

Figure 3 Standard Gibbs free energy of (a) Zn (s, g) + $\frac{1}{2}O_2$ (g) $\rightleftharpoons$ ZnO (s); (b) H_2 (g) + $\frac{1}{2}O_2$ (g) $\rightleftharpoons$ H_2O (g); (c) ZnO (s) + H_2 (g) $\rightleftharpoons$ Zn (s, g) + H_2O (g).

Fig. 3 shows the standard Gibbs free energies of reaction 1 and of the following reactions:

$$H_2\,(\text{gas}) + \tfrac{1}{2}O_2\,(\text{gas}) \rightleftharpoons H_2O\,(\text{gas}) \qquad (3)$$

$$ZnO\,(\text{solid}) + H_2\,(\text{gas}) \rightleftharpoons Zn\,(\text{solid, gas}) + H_2O\,(\text{gas}) \qquad (4)$$

The relevant thermochemical data are given in Table II. It may be seen from Fig. 3 that reduction of ZnO to metallic Zn by pure hydrogen at one atmospheric pressure is possible only above 1560 K (corresponding to $pO_2 = 1.626 \times 10^{-11}$ atmosphere); below this temperature ZnO (solid) is more stable (less free energy) than H_2O (gas).

The melting point of ZnO is 2243 K, and it decomposes before boiling. The vapour pressure of ZnO at its melting point is very low. Unlike ZnO, the melting point of $ZnCl_2$ is fairly low (591 K), and the vapour pressure of molten zinc chloride increases almost exponentially with increasing temperature (Fig. 4). It may be noted that zinc chloride vaporizes as monomeric $ZnCl_2$ and dimeric Zn_2Cl_4 species; however, the vapour pressure of the dimeric species is much smaller relative to that of the monomeric species.

TABLE II Standard Gibbs free energies of the reactions (in calories)

Zn (solid) + $\frac{1}{2}O_2$ (gas) $\rightleftharpoons$ ZnO (solid)		(1)
Zn (gas) + $\frac{1}{2}O_2$ (gas) $\rightleftharpoons$ ZnO (solid)		(1a)
H_2 (gas) + $\frac{1}{2}O_2$ (gas) $\rightleftharpoons$ H_2O (gas)		(3)
ZnO (solid) + H_2 (gas) $\rightleftharpoons$ Zn (solid) + H_2O (gas)		(4)
ZnO (solid) + H_2 (gas) $\rightleftharpoons$ Zn (gas) + H_2O) (gas)		(4a)
ΔG_1°	$= -84100 - 6.9T\log T + 44.14T$	(298–693 K)
ΔG_{1a}°	$= -115420 - 10.35T\log T + 82.38T$	(1170–2000 K)
ΔG_3°	$= -58900 + 13.1T$	(298–2500 K)
ΔG_4°	$= 25200 + 6.9T\log T - 31.04T$	(298–693 K)
ΔG_{4a}°	$= 56520 + 10.35T\log T - 69.28T$	(1170–2000 K)

Fig. 5 shows the standard Gibbs free energy of formation of $ZnCl_2$ (solid, liquid, gas) and $AlCl_3$ (gas) and Al_2Cl_6 (gas). The relevant thermochemical data are given in Table III. It is interesting to note that at

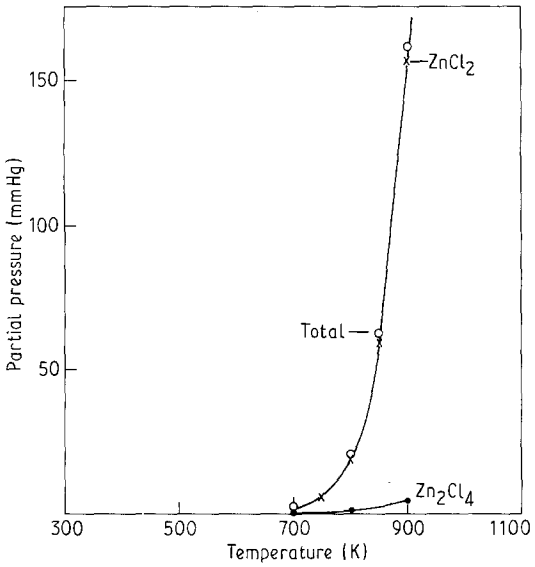

Figure 4 Equilibrium vapour pressure of $ZnCl_2$ at different temperatures.

all temperatures between 453 and 932 K (mp of Al), $AlCl_3$ (gas) is more stable than $ZnCl_2$ (solid, liquid); and dimeric Al_2Cl_6 (gas) is more stable even than $AlCl_3$ (gas). However, at temperatures above 1200 K, when zinc, chlorine and zinc chloride are all in the gaseous state, the standard Gibbs free energy of formation of $ZnCl_2$ (gas) is only slightly lower than that of $AlCl_3$ (gas). Thermochemical data for Al_2Cl_6 (gas), the stablest form of aluminium chloride, are not available; but from the trend of the results it is expected that Al_2Cl_6 (gas) will be more stable than $ZnCl_2$ (gas) even above 1200 K.

The melting point of Al is 932 K, and its vapour pressure, even in the molten state, is very low (boiling point at 2723 K). However, $AlCl_3$ and Al_2Cl_6 sublimate under one atmospheric pressure, and their vapour pressures, particularly of Al_2Cl_6, are very high (Fig. 6). Thus attempts to make aluminium-doped ZnO film by spray pyrolysis of solutions containing chloride, particularly if aluminium is added to the solution as aluminium chloride, do not seem to be promising. This is particularly because the rate of hydrolysis of aluminium chloride in aqueous solution at room temperature is very slow [19].

3.2. Thermal analysis

Fig. 7 shows the differential thermal analysis (DTA) and thermogravimetric (TG) curves of zinc acetate, which crystallizes as $Zn(CH_3COO)_2 \cdot H_2O$ from aqueous solution at room temperature. On heating, the water of crystallization is lost around 100 °C; this is indicated on the DTA curve as a symmetrical endothermic peak and about 16% weight loss on the TG curve. This is followed by a sharp endothermic peak around 240 °C, probably due to melting of anhydrous zinc acetate. Another possible reason for this endothermic peak around 240 °C may be the pyrolytic decomposition of zinc acetate to zinc oxide and acetic anhydride, followed by loss of acetic anhydride (bp 140 °C). Since the DTA peak at 240 °C is also accompanied by a weight loss of 54%, as indicated on the TG curve, the second alternative seems to be more probable. The broad exothermic DTA peak around 320 °C, which involves no change in weight of the sample, may be due to some sluggish structural changes of ZnO. The usual crystal structure of zinc oxide is hexagonal close-packed of the wurtzite type with two significant characteristics: large extra ionic volume with relatively large voids (0.095 nm), and regular alternating layers of zinc and oxygen in the direction of the c axis [20, 21]. An alternative form of zinc oxide is a face-centred lattice corresponding to the zinc blend type usually formed in thin films [22].

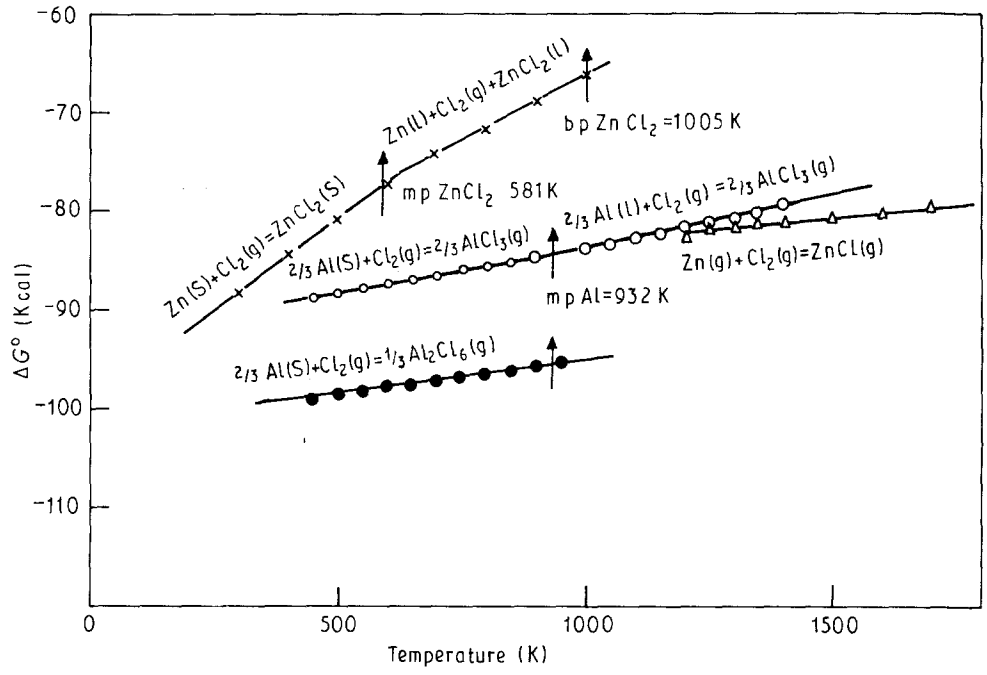

Figure 5 Standard Gibbs free energy of (a) Zn (s, l, g) + Cl_2 (g) $\rightleftharpoons$ $ZnCl_2$ (s, l, g); (b) $\frac{2}{3}$Al (s, l) + Cl_2 (g) $\rightleftharpoons$ $ZnCl_2$ (s, l, g); (c) $\frac{2}{3}$Al (s, l) + Cl_2 (g) $\rightleftharpoons$ $\frac{1}{3}Al_2Cl_6$ (g).

TABLE III Standard Gibbs free energies of the reactions (in calories)

Zn (solid)	$+ Cl_2$ (gas) $\rightleftharpoons ZnCl_2$ (solid)	(5)
Zn (solid, liquid)	$+ Cl_2$ (gas) $\rightleftharpoons ZnCl_2$ (liquid)	(5a)
Zn (gas)	$+ Cl_2$ (gas) $\rightleftharpoons ZnCl_2$ (gas)	(5b)
2/3 Al (solid)	$+ Cl_2$ (gas) $\rightleftharpoons \frac{2}{3} AlCl_3$ (gas)	(6)
2/3 Al (liquid)	$+ Cl_2$ (gas) $\rightleftharpoons \frac{2}{3} AlCl_3$ (gas)	(6a)
2/3 Al (solid)	$+ Cl_2$ (gas) $\rightleftharpoons \frac{1}{3} Al_2Cl_6$ (gas)	(7)

ΔG_5°	$= -101\,385 - 12.85T \log T + 75.45T$	(298–586 K)
ΔG_{5a}°	$= -93\,950 + 27.35T$	(586–1005 K)
ΔG_{5b}°	$= -93\,800 - 9.44T \log T + 38.6T$	(1180–1800 K)
ΔG_6°	$= -92\,107 + 1.6533T \log T + 3.1667T$	(453–932 K)
ΔG_{6a}°	$= -93\,600 + 1.6667T \log T + 4.7T$	(932–1400 K)
ΔG_7°	$= -101\,467 + 1.65T \log T + 1.41T$	(453–932 K)

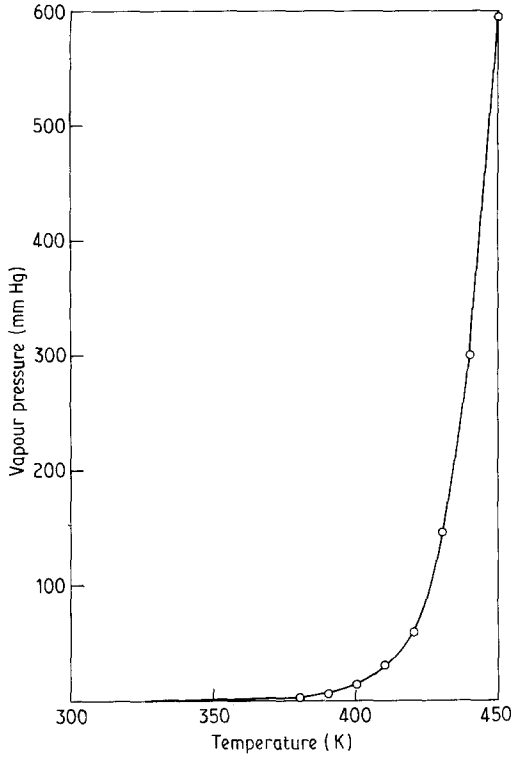

Figure 6 Equilibrium vapour pressure of $AlCl_3$ and Al_2Cl_6.

Formation of zinc carbonate as an intermediate during pyrolysis, as is the case with basic oxides of Ba, Sr etc. during pyrolysis of their metal salts of carboxilic acids [23] is not possible because $ZnCO_3$ decomposes at low temperatures ($\sim 300\,^\circ C$), and is metastable even at room temperature. The standard Gibbs free energy of the reaction

$$ZnCO_3 \text{ (solid)} \rightleftharpoons ZnO \text{ (solid)} + CO_2 \text{ (gas)} \quad (5)$$

has been calculated with available thermochemical

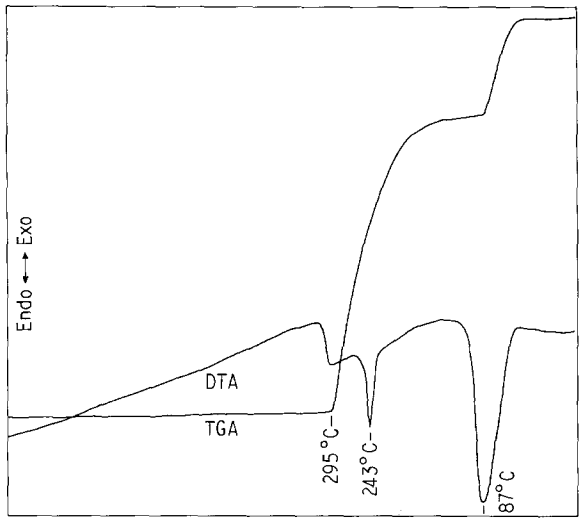

Figure 7 Thermogram of zinc acetate hydrate.

data (given in Table IV), and is shown plotted in Fig. 8. The equilibrium thermodynamic pCO_2 of reaction 5 has been calculated and is shown in Fig. 9 as function of temperature. It may be seen that significant pCO_2 (~ 10 mm Hg) develops over $ZnCO_3$ at a temperature as low as 300 K (27 °C). A typical thermogram of 'zinc carbonate' prepared in our laboratory is shown in Fig. 10. This zinc carbonate was produced by dissolving 2.00 g of pure ZnO in dilute nitric acid followed by addition of excess solid Na_2CO_3. The precipitate was allowed to stand in the mother liquor for 24 h, followed by filtration, washing thoroughly with deionized water and finally with dry ethyl alcohol. The alcohol-washed powder was dried in a vacuum desiccator for 4 h. From X-ray analysis, the powder was identified as basic zinc carbonate: $2ZnCO_3 \cdot 3Zn(OH)_2 \cdot H_2O$. The thermogram of Fig. 10 shows an endothermic medium height peak accompanied by single stage weight loss from room temperature to 135 °C (maximum of DTA curve is at 95 °C); this is due to the loss of one molecule of water of crystallization. This is followed by a large endothermic peak in the temperature range 135 to 240 °C accompanied by a single-stage weight loss. This is undoubtedly due to decomposition of $ZnCO_3$ and $Zn(OH)_2$ to ZnO. However, whether these two decompositions occur independently and simultaneously could not be ascertained from the present study. The weight of the sample becomes steady and no thermal changes occur on further heating of the sample up to 700 °C.

It is interesting to note that the two stages of decomposition of basic zinc carbonate, as mentioned

TABLE IV Standard Gibbs free energy of the reaction $ZnCO_3$ (solid) = ZnO (solid) + CO_2 (gas) and relevant thermochemical data

H_{298}°

$ZnCO_3$ (solid)	$= -194\,200$ cal mol^{-1}
ZnO (solid)	$= -83\,200$ cal mol^{-1}
CO_2 (gas)	$= -94\,050$ cal mol^{-1}

S_{298}°

$ZnCO_3$ (solid)	$= 19.7$ cal mol^{-1} °C^{-1}
ZnO (solid)	$= 10.4$ cal mol^{-1} °C^{-1}
CO_2 (gas)	$= 51.1$ cal mol^{-1} °C^{-1}

C_P°

$ZnCO_3$ (solid)	$= 9.30 + 33.0 \times 10^{-3}T$
ZnO (solid)	$= 11.71 + 1.22 \times 10^{-3}T - 2.18 \times 10^5 \times T^{-2}$
CO_2 (gas)	$= 10.55 + 2.16 \times 10^{-3}T - 2.04 \times 10^5 \times T^{-2}$

$$\Delta G_T^\circ = -789.18 - 12.96T \ln T + 80.3435T + 14.81 \times 10^{-3} \times T^2 + 2.11 \times 10^5 \times T^{-1}$$

above, involve the following weight changes:

$$2ZnCO_3 \cdot 3Zn(OH)_2 \cdot H_2O \xrightarrow[-3.17\ wt\ \%]{H_2O} 2ZnCO_3 \cdot 3Zn(OH)_2$$

$$-28.22\ wt\ \% \downarrow -(3H_2O + 2CO_2)$$

$$5ZnO$$

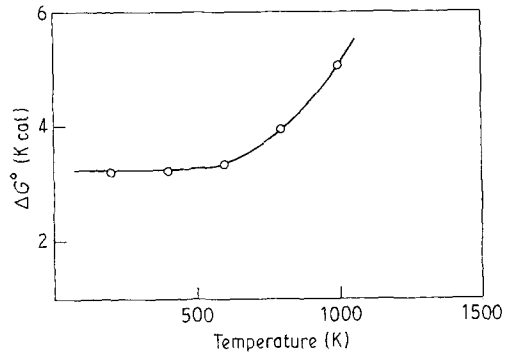

Figure 8 Standard Gibbs free energy of the reaction $ZnCO_3$ (s) $\rightleftharpoons$ ZnO (s) + CO_2 (g).

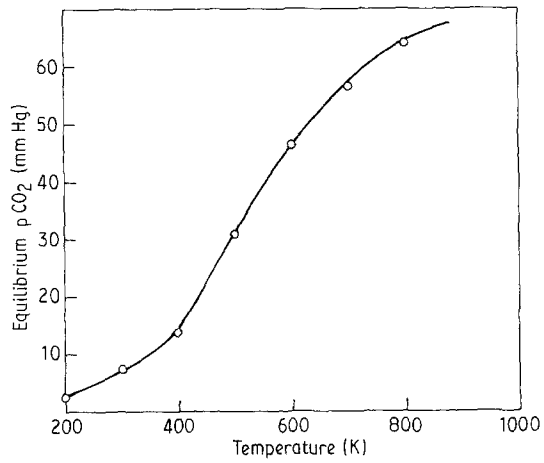

Figure 9 Equilibrium partial pressure of CO_2 over $ZnCO_3$ (s) at different temperatures.

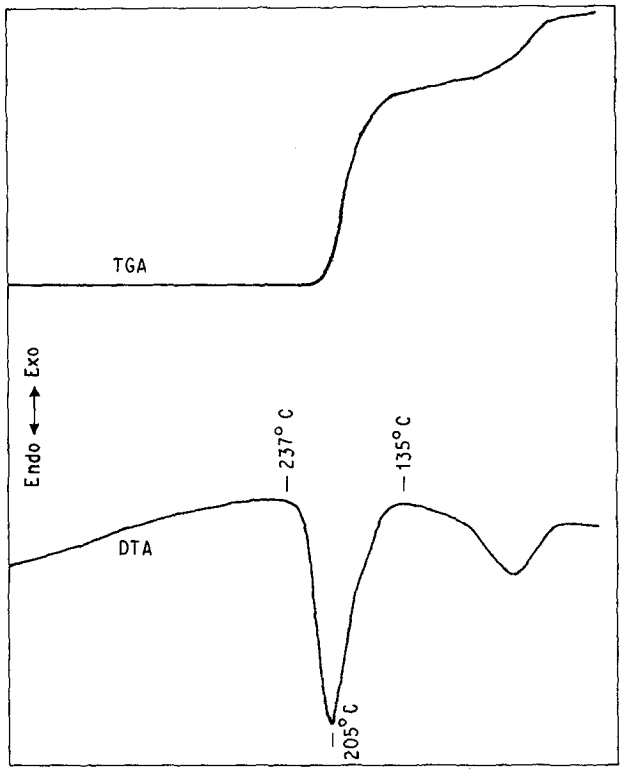

Figure 10 Thermogram of basic zinc carbonate.

and the actual weight changes that occur (as seen on the TG curve) are 3.5 and 28.0 wt %, respectively. The thermogram of zinc acetate containing zinc chloride is similar to that of zinc acetate hydrate, except that a sharp endothermic peak occurs on the DTA curve around 320 °C due to melting of zinc chloride (mp of $ZnCl_2$ is 318 °C).

4. Conclusions

1. Zinc acetate pyrolyses to ZnO without any intermediate carbonate formation; the conversion becomes complete at 350 °C.

2. ZnO cannot be reduced to metallic Zn even by pure hydrogen at one atmospheric pressure at temperatures lower than 1287 °C (1560 K).

3. Zinc chloride is more stable than zinc oxide. Thus the presence of chlorine (chloride) during pyrolysis will convert zinc oxide to zinc chloride; and a significant amount of zinc will be lost through volatilization as zinc chloride.

4. Aluminium chloride (Al_2Cl_6) hydrolyses very slowly in aqueous solution. Since the sublimation temperature of Al_2Cl_6 is very low (~ 160 °C), aluminium doping of ZnO using aluminium chloride in the spray solution is not expected to produce satisfactory results.

References

1. M. TAKATA, D. TSUBONE and H. YANAGIDA, *J. Amer. Ceram. Soc.* **59** (1975) 4.
2. E. W. GORTER, *Proc. IRE* **43** (1955) 1945.
3. A. Y. CORAN, in "Science and Technology of Rubber", edited by F. R. Eirich (Academic Press, New York, 1978) ch. VII.
4. E. A. GIESS, *J. Amer. Ceram. Soc.* **47** (1964) 388.
5. A. SIMON, C. OEHME and K. POHL, *Anorg. Allgem. Chem.* **314** (1962) 61.
6. *Idem., ibid.* **317** (1962) 230.
7. *Idem., ibid.* **323** (1963) 160.
8. D. E. RASE and F. H. DOLIN, *J. Amer. Ceram. Soc.* **43** (1960) 125.
9. S. F. BARTRAM and R. A. SLEPETYS, *Trans. Amer. Ceram. Soc.* **44** (1961) 493.
10. A. R. HUTSON, *Phys. Rev. Lett.* **4** (1960) 505.

11. W. WEBB, D. W. WILLIAMS and M. BUCHANAN, *Appl. Phys. Lett.* **39** (1981) 640.
12. T. MINAMI, H. NANTO and S. TAKATA, *ibid.* **41** (1982) 958.
13. M. NEUBERGER, OTS AD425212 (US Government Printing Office, Washington, D.C., 1963).
14. T. J. GRAY and P. AMIGUE, *Surf. Sci.* **13** (1969) 209.
15. T. J. GRAY, in "High Temperature Oxides", Part. IV, "Refractory Glasses, Glass-Ceramics, and Ceramics" edited by A. M. Alper (Academic Press, New York, 1971) p. 138.
16. J. S. ANDERSON, *Ann. Rep. Chem. Soc.* **43** (1947) 110.
17. H. H. BAUMBACK and C. WAGNER, *Z. Phys. Chem.* **22** (1933) 199.
18. F. VAN CRAEYREST, W. MAENHOUT-van der VORST and W. DEKEYSER, *Phys. Status Solidi* **8** (1965) 841.
19. J. AVESTON, *J. Chem. Soc.* **87** (1965) 4438.
20. R. W. G. WYCKOFF, in "Crystal Structure", 2nd edn. (Wiley, New York, 1963).
21. A. N. MARIANO and R. E. HANNEMAN, *J. Appl. Phys.* **34** (1963) 384.
22. W. L. BRAGG and J. A. DARBYSHIRE, *Trans. Faraday Soc.* **28** (1932) 522.
23. M. MANEVA and D. NIKOLOVA, *J. Ther. Analysis* **34** (1988) 637.

Received 28 November 1990
and accepted 10 April 1991